

TRANSVERSE-EMITTANCE PRESERVING TRANSFER LINE AND ARC COMPRESSOR FOR HIGH BRIGHTNESS ELECTRON SOURCES*

S. Di Mitri[#], M. Cornacchia, Elettra Sincrotrone Trieste, 34149 Basovizza, Trieste, Italy
 S. Spampinati, Department of Physics, University of Liverpool, Liverpool L69 7ZX, United Kingdom, and Cockcroft Institute, Sci-Tech Daresbury, Warrington WA4 4AD, United Kingdom

Abstract

Minimizing transverse emittance is essential in single- or few-passes accelerators designed to deliver high brightness electron beams. Emission of coherent synchrotron radiation (CSR) is an important factor of emittance degradation. We have demonstrated, with analytical and experimental results, that this perturbation may be cancelled by imposing certain conditions on the electron optics when the bunch length is constant along the line. This scheme of CSR suppression is then enlarged, analytically and numerically, to cover the case of varying bunch length in a periodic arc compressor. The proposed solution holds the promise of cost-saving of compact transfer lines with large bending angles, and new schemes for beam longitudinal gymnastics both in recirculating and in single-pass accelerators driving free electron lasers.

INTRODUCTION

The advent of sub-ps electron beams with very high brightness in free electron lasers (FELs) [1] and in linear colliders has raised the awareness of the accelerator community to the effect of the coherent synchrotron radiation (CSR) on beam transverse emittance [2–5]. The CSR field affects the electron transverse motion both with radial forces and by changing the particle energy in the dispersive line. In the latter case, the particle starts a betatron oscillation around a new reference trajectory, thus increasing its Courant-Snyder (C-S) invariant [6]. The synchrotron radiation emission is coherent for wavelengths comparable to the electron bunch length and it induces a variation of the particle energy that is correlated with the longitudinal coordinate along the bunch. The removal of that correlation may therefore suppress the CSR-driven emittance growth [7,8].

In the following, we show that linear optics formalism can be used to describe the effect of consecutive *identical* CSR energy kicks on the beam transverse emittance; CSR emission is assumed to happen in the 1-D (longitudinal) and steady-state approximation [9]. The analytical prediction for the final emittance as function of the optics setting in a substantially isochronous transfer line was validated experimentally in the FERMI FEL [10,11] high energy Spreader line [12]. We then show that the same formalism can be extended to the case of a non-isochronous beam line, made of several large-angle dipole magnets, with limited impact on the beam emittance [13].

*Work supported by the FERMI project and the ODAC project of Elettra Sincrotrone Trieste.
[#]simone.dimitri@elettra.eu

ISOCHRONOUS LINE

The FERMI achromatic system, denoted henceforth as Spreader, is made of two identical double bend achromats (DBA), as sketched in Fig.1. Each DBA includes two FODO cells and their nominal setting ensures $\Delta\mu = \pi$ between the dipoles, and symmetric Twiss functions β and α , with values β_1 (α_1) and β_4 (α_4) in the dipoles of the first and the second achromat, respectively. The two DBAs are separated by 7 quadrupoles with a phase advance of π between them. In the following, the C-S formalism is applied to the particle motion in the Spreader with the aforementioned notation. Only the motion in the bending plane is considered.

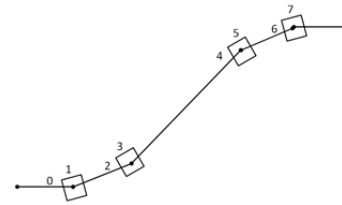


Figure 1: Sketch of the FERMI Spreader (not to scale). The design optics gives a betatron phase advance of π in the bending plane between two consecutive dipoles. There are quadrupoles between the dipoles (not shown here). Copyright of American Physical Society [12].

The initial particle coordinates relative to the reference trajectory are $x_0 = 0, x'_0 = 0$ and the initial particle C-S invariant is $2J_0 = 0$. The variable subscript refers to the point along the lattice, as indicated in Fig.1. After the CSR kick in the first dipole, the particle transverse coordinates become:

$$\begin{cases} x_1 = \eta\delta \equiv \sqrt{2J_1\beta_1} \cos\Delta\mu|_{\Delta\mu=0} = \sqrt{2J_1\beta_1} \\ x'_1 = \eta'\delta \equiv -\frac{\sqrt{2J_1}}{\beta_1} (\alpha_1 \cos\Delta\mu + \sin\Delta\mu)|_{\Delta\mu=0} = -\alpha_1 \sqrt{\frac{2J_1}{\beta_1}} \end{cases} \quad (1)$$

Here δ is the single particle relative energy deviation induced by CSR. After the CSR kick, the particle C-S invariant has grown to

$$2J_1 = \gamma_1 x_1^2 + 2\alpha_1 x_1 x'_1 + \beta_1 x_1'^2 = H_1 \delta^2, \quad \text{where}$$

$$H_1 = \gamma_1 \eta^2 + 2\alpha_1 \eta \eta' + \beta_1 \eta'^2 \text{ and } \gamma_1 = \left(\frac{1 + \alpha_1^2}{\beta_1} \right). \quad \text{At the}$$

second dipole, after π phase advance and in the presence of the second CSR kick, we have:

$$\begin{cases} x_3 = x_2 + \eta\delta = -\sqrt{2J_1\beta_2} + \sqrt{2J_1\beta_1} = 0 \\ x'_3 = x'_2 - \eta'\delta = \alpha_2\sqrt{\frac{2J_1}{\beta_2}} + \alpha_1\sqrt{\frac{2J_1}{\beta_1}} = \sqrt{\frac{2J_1}{\beta_1}}(\alpha_1 + \alpha_2) \end{cases} \quad (2)$$

Equation 2 was obtained by substituting the dispersive terms as in Eq.1 and by using the symmetry of β at the dipoles (no specific choice for α is made at this stage). The same steps followed so far can easily be repeated till the end of the line. A new invariant will be defined after each CSR kick by the algebraic addition of the dispersive terms to the particle coordinates. With the additional equality $2J_i = \gamma_i x_i^2 + 2\alpha_i x_i x'_i + \beta_i x_i'^2$ for $i = 3, 5, 7$, each invariant J_i will be expressed as a function of J_1 and the C-S parameters. Doing this, after the last CSR kick we obtain:

$$2J_7 = 2J_1 4\alpha_1^2 \left(1 - \sqrt{\frac{\beta_5}{\beta_1}}\right)^2 \equiv 2J_1 X_{17}, \quad (3)$$

with the prescription $2J_1 = H_1 \delta^2$, $\sigma_{\delta, CSR}^2 = \langle \delta_{CSR}^2 \rangle$, we estimate a residual emittance growth at the Spreader's end:

$$\Delta\gamma\varepsilon = \gamma\varepsilon \left[\sqrt{1 + \frac{H_1 \sigma_{\delta, CSR}^2}{\varepsilon} X_{17}} - 1 \right] < 0.1 \mu\text{m}, \quad (4)$$

where ε is the unperturbed geometric emittance and γ is the relativistic Lorentz factor for the beam mean energy. The experimental demonstration of cancellation of CSR kicks, i.e. $X_{17} = 0$ in Eq.4, is shown in Fig.2.

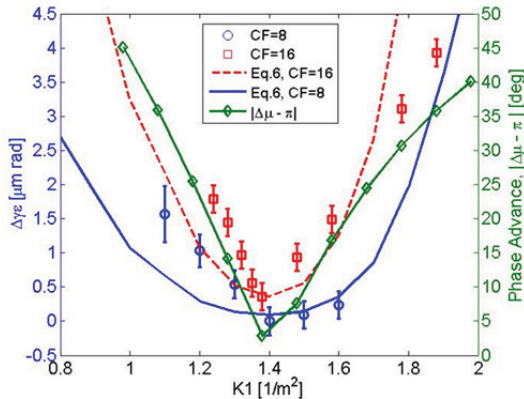


Figure 2: Horizontal normalized emittance growth at the end of the Spreader (markers with error bars) as a function of the strength of a quadrupole placed between the two DBAs. The squares (circles) are for a bunch length compression factor CF=16 (8) carried out in the upstream linac. The horizontal betatron phase advance between the DBAs (diamonds) was computed with ELEGANT on the basis of the experimental machine settings; the absolute value of its distance from π is shown. The dashed (solid) line is the evaluation of Eq.4 for CF=16 (8). Copyright of American Physical Society [12].

The emittance growth was measured at the end of the Spreader as the phase advance between the two achromats and the C-S parameters in the second achromat were changed by varying a quadrupole's strength in the intermediate dispersion-free region, thus breaking the optics balance. The perturbed optics was computed for each quadrupole's strength with the ELEGANT code [14], and thereby used to evaluate Eq.4. The experimental growth rate was higher for the shorter beam, in agreement with the expected CSR dynamics and well described by the analytical model. Minimum emittance growth was achieved for a π phase advance between the two achromats and design C-S parameters at the second achromat, again in agreement with the theoretical expectation.

It is worth mentioning that the expression for the CSR kick in Eq.1 was recently re-modelled in [15] with a more accurate expression that takes into account a non-zero length of the dipole magnets. That modeling was shown to provide a more accurate control of the final beam emittance, and an exact solution for the optical cancellation of the CSR-induced invariant in a single symmetric DBA.

NON-ISOCRONOUS LINE

Bunch length magnetic compression is routinely used in high brightness electron linacs driving FELs and particle colliders in order to shorten the bunch that is to increase the peak current of the injected beam from few tens to kilo-Amperes. To date, magnetic compression is performed in dedicated non-isochronous insertions made of few degrees bending magnets inserted on the accelerator straight path; the compression factor is limited by the degradation of the beam transverse emittance owing to emission and absorption of CSR. For this reason, if a high peak current is needed, for instance, at the end of recirculating accelerators like energy-recovery linacs (ERLs) driving FEL, the photo-injected beam is recirculated in isochronous beam lines and magnetically time-compressed only after the very last stage of acceleration [16], e.g. with a magnetic chicane [17,18]. Although this approach tends to preserve beam brightness during recirculation [19], it may put an upper limit to either the compression factor or the beam charge or both, thus to the final peak current, because of CSR-induced emittance growth in a single-stage compression [20].

In the following, we reformulate the concept introduced above of CSR-driven optics balance [12] for the more general case of varying bunch length [13], and show that it works for bending angles larger than previously thought advisable and practical. The proposed solution applies adiabatic compression throughout the arc. Optical aberrations and longitudinal nonlinearities are controlled with sextupole magnets. We show that it is feasible to redistribute a compression factor of up to 45 for a 500 pC beam, by means of a periodic 180 deg arc at 2.4 GeV, while keeping CSR transverse kicks under control. The total growth of the normalized emittance does not exceed

the 0.1 μm level for peak currents of up to 2 kA. In comparison with existing literature [21–24], our solution allows larger compression factors at higher charges, and simplifies ERL lattice designs since, in principle, a dedicated chicane is no longer needed for compression as the arc acts both as final stage of recirculation and compressor. Although it finds an immediate application to ERLs, the proposed CSR-immune arc compressor promises to be applicable to more general accelerator design, thus offering the possibility of new and more effective layout geometries of single-pass accelerators and of new schemes for beam longitudinal gymnastic.

The 180 deg arc compressor is made of 6 modified Chasman-Green achromats (one cell shown in Fig.3; linear optics functions in Fig.4) separated by drift sections that allow optics matching from one DBA to the next one. The arc is 125 m long (40 m long radius) and functional up to 2.4 GeV. The bending angle per sector dipole magnet is $\theta = 0.2618$ rad and the dipole arc length $l_b = 1.4489$ m. R_{56} of one dipole is 17.2 mm, while that of the entire arc is 207.1 mm. If, for example, a total compression factor $C = 45$ were required at the end of the arc, an energy chirp $h = \left(\frac{1}{C} - 1\right) \frac{1}{R_{56}} \approx 4.7 \text{ m}^{-1}$ would be

needed at its entrance, which corresponds roughly to a fractional rms energy spread of $\sigma_{\delta,0} \approx h \sigma_{z,0} = \frac{1}{E} \frac{dE}{dz} \sigma_{z,0} \approx 0.3\%$ for a 3 ps rms long bunch.

According to the analysis depicted above, the normalized emittance growth in the bending plane and in the presence of CSR for a *single* DBA cell can be estimated by:

$$\Delta \varepsilon_{nf} = \varepsilon_{nf} - \varepsilon_{n0} \cong \varepsilon_{n0} \left(\sqrt{1 + \frac{\gamma J_3}{\varepsilon_{n0}}} - 1 \right), \quad (5)$$

where the single particle C-S invariant $2J_3$ is:

$$2J_3 = \beta_2 x_3'^2 + 2\alpha_2 x_3 x_3' + \left(\frac{1 + \alpha_2^2}{\beta_2} \right) x_3^2 \quad (6)$$

$$\cong \left(\frac{k_1 \rho^{1/3} \theta^2}{2} \right)^2 \left\{ \left[\sqrt{\beta_2} (C^{4/3} + 1) - \frac{\alpha_2}{\sqrt{\beta_2}} \left(\frac{l_b}{6} \right) (C^{4/3} - 1) \right]^2 + \left[\frac{1}{\sqrt{\beta_2}} \left(\frac{l_b}{6} \right) (C^{4/3} - 1) \right]^2 \right\}$$

It is worth noticing that $(k_1 \rho^{1/3} \theta)$ in Eq.6 is the rms value of the fractional energy spread induced by CSR in the first dipole magnet of a DBA cell, and that its evolution along the cell (thus the arc), as well as that of the bunch length, is taken into account by the cell compression factor C . The invariant has a minimum for

$$\beta_2 \cong \beta_{2,\min} = \frac{l_b}{6} \left(\frac{C^{4/3} - 1}{C^{4/3} + 1} \right); \quad \beta_2 \text{ is the betatron function}$$

inside the dipole magnet, where the beam size is forced to a waist, and l_b is the dipole's length. In the lattice under

consideration we expect to have minimal CSR effect on the emittance for $\beta_{2,\min} \sim 0.2$ m.

In summary, in order to minimize the CSR-induced emittance growth in a periodic 180 deg arc compressor, we prescribe the use of several symmetric DBA cells with linear compression factor not far from unity in most of the cells. We also impose a beam waist in the dipoles of all the DBAs and find that, unlike in a magnetic chicane (see [25] and references therein), there is an optimum value for β_2 inside the dipoles that minimizes the chromatic emittance growth due to CSR.

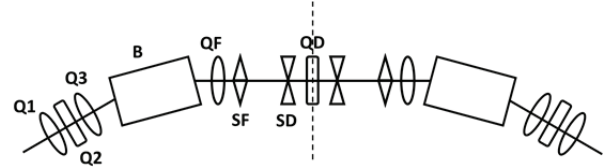


Figure 3: Sketch (not to scale) of the arc compressor DBA cell. Dipole magnets (B), focusing (QF, Q1 and Q3) and defocusing (QD, Q2) quadrupole magnets, focusing (SF) and defocusing sextupole magnets (SD) are labelled. The geometry and the magnets' arrangement is symmetric with respect to the middle axis (dashed line). Copyright of Europhysics Letters [13].

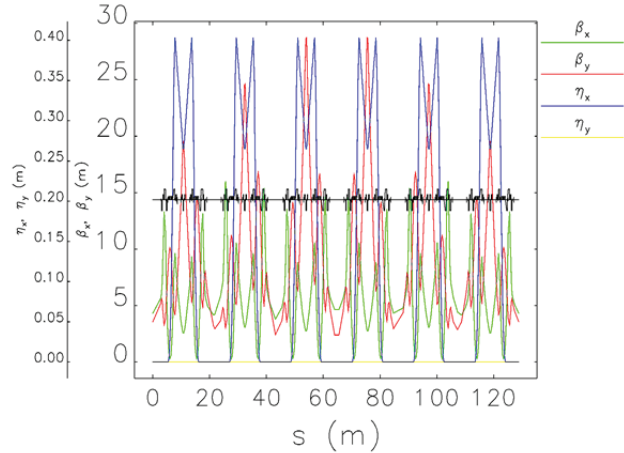


Figure 4: Linear optics functions along the 180 deg arc compressor. Optics functions are quasi-symmetric in each DBA cell of the arc compressor, and totally symmetric with respect to the middle axis of the arc. The minimum β_x is in the dipole magnets, and it ranges from 0.14 m to 0.26 m over the six cells.

Table 1 summarizes the arc input and output beam parameters used in ELEGANT particle tracking runs. Two sets of initial beam parameters are considered, one for high charge–long bunch, the other for low charge–short bunch. Five million particles in a bunch were tracked. Quiet start of the electron beam input distribution and filtering were adopted to ensure suppression of numerical sampling noise at uncompressed wavelengths shorter than 35 μm . The rms normalized projected emittance of the

500 pC beam grows from $0.80 \mu\text{m}$ to $1.05 \mu\text{m}$ at the arc's end, with contributions from incoherent synchrotron radiation (ISR), chromatic aberrations and CSR, as shown in Fig.5. Chromatic aberrations are responsible for the emittance modulation along the line, as well as for the (small) horizontal slice emittance growth, shown in Fig.6-top plot. Non-uniformity of the horizontal C-S slice invariant (i.e., the invariant of the slice centroid) along the bunch, shown in Fig. 6-bottom plot, reflects the slices misalignment in the transverse phase space due to CSR kicks. Residual CSR-induced microbunching shows up in the longitudinal phase space at final wavelengths longer than $10 \mu\text{m}$. Final slice energy spread is around 2 MeV and substantially dominated by the initial uncorrelated energy spread times the total compression factor.

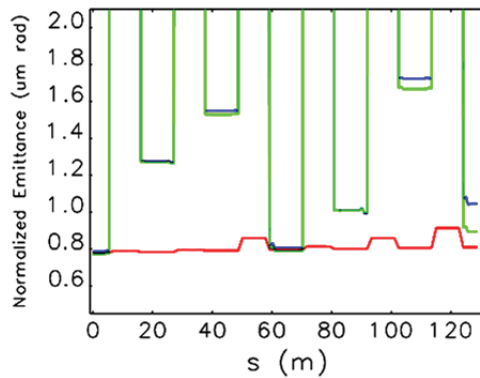


Figure 5: Projected normalized emittance (rms value) in the bending plane along the arc, for the 500 pC beam (see Table 1). The emittance evolution is shown, respectively, in the presence of ISR-only for the fully compressed beam (red), with the addition of compression and optical aberrations (green) and with the further addition of CSR (blue). Copyright of Europhysics Letters [13].

Table 1. Electron Beam Parameters at the Entrance and at the Exit of the Arc Compressor (Simulation Results). Rms values are computed over 100% of the beam charge. Input values are only indicative and do not necessarily reflect optimized beams from the injector

Input beam			
Energy	2.4	2.4	GeV
Charge	100	500	pC
Bunch length, rms	300	900	μm
Peak current	30	45	A
Proj. norm. emittance, rms	0.20,0.20	0.80,0.80	$\mu\text{m rad}$
Uncorr. energy spread, rms	30	40	keV
Corr. energy spread, rms	0.14	0.42	%
Output beam			
Compression factor	45	45	
Peak current	1400	2000	A
Proj. norm. emittance, rms	0.34, 0.23	1.05, 0.82	$\mu\text{m rad}$
Slice energy spread, rms	≤ 1.6	≤ 2.0	MeV
CSR energy spread, rms	0.003	0.003	%

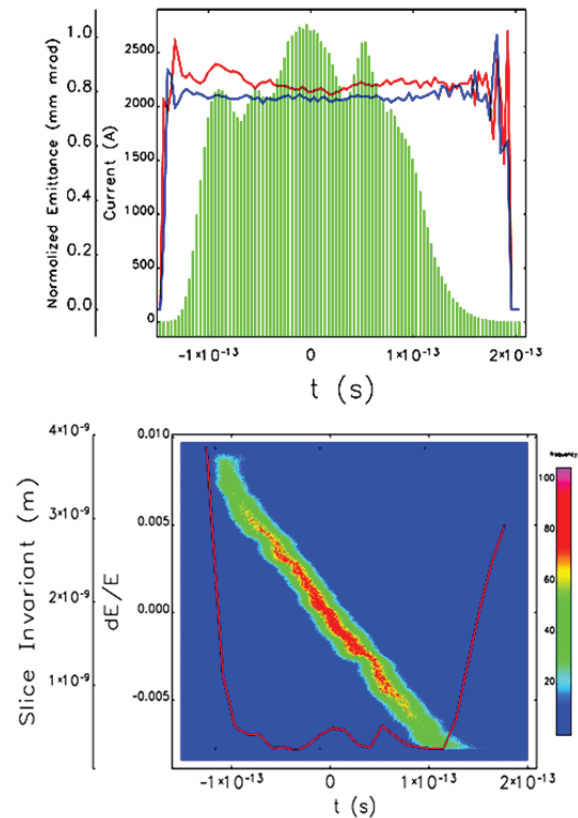


Figure 6: Top: current profile (histogram), superimposed to the slice rms normalized emittance. Bottom: longitudinal phase space, superimposed to the slice Courant-Snyder invariant (solid line): the horizontal one varies along the bunch because of CSR kicks. Bunch head is at negative time coordinates. Copyright of Europhysics Letters [13].

FINAL REMARKS

The capability of controlling CSR effects in an arc compressor (not necessarily constrained to a 180 deg total bending angle) – and thus to increase the beam peak current while preserving its 6-D normalized brightness using an approach that goes beyond those offered by the existing literature – quite generally opens the door to new geometries in accelerator design and new schemes of beam longitudinal gymnastic. For example, after single- or multi-pass acceleration in an FEL linac-driver, the beam can be arc-compressed at high energy and counter-propagated into an undulator, which could then lie parallel to the accelerator. At least two advantages are seen: one is that cost savings are achieved in civil construction, the other is that the operation of the system is simplified, as much as the beam does not undergo any manipulation other than acceleration until it reaches the arc compressor. On the basis of our findings, the arc could be investigated as either compressor (together with a proper setting of the upstream RF phases to match the arc's positive R_{56}) or a CSR-immune transfer line, if the beam has no energy chirp at its entrance. Our arc compressor design is also recommended for an ERL, or recirculated linac-driven FEL such as that described in [26]. In this case, the

electron beam may be accelerated and recirculated in isochronous beam lines until it reaches the target energy and energy chirp, and eventually compressed. From the entrance to the exit of the arc compressor, the energy spread, normally dominated by the energy chirp, remains substantially unchanged. In order for the FEL amplification process to be efficient, σ_δ must be matched to the normalized FEL energy bandwidth, ρ [27]. For lasing in x-rays, $\rho \geq 10^{-4}$ and this may require a removal of the energy chirp downstream of the arc, i.e. with a dedicated RF section. With the 500 pC beam parameters of Table 1, we estimate [28] lasing at 1.3 nm with $\rho = 1.1 \times 10^{-3}$, a 2.1 m-long 3-D gain length, and FEL power saturating at 2.6 GW in a 36 m long undulator.

ACKNOWLEDGEMENTS

The authors are grateful to D.R. Douglas for encouragements and fruitful discussions on arcs design, and to Y. Jiao for discussions on emittance control in DBAs. The authors are also in debt to the FERMI Team for their support in running the machine and for the development of the diagnostic tools that permitted the analysis of the experimental observations at FERMI. This work has been funded by the FERMI project and the ODAC project of Elettra Sincrotrone Trieste.

REFERENCES

- [1] S. Di Mitri, M. Cornacchia, *Physics Reports* **539** (2014) 1-48.
- [2] R. Talman, *Phys. Rev. Lett.* **56**, 1429 (1986).
- [3] T. Nakazato et al., *Phys. Rev. Lett.* **63**, 2433 (1989).
- [4] Ya.S. Derbenev, J.Rossbach, E.L. Saldin, and V.D. Shiltsev, TESLA-FEL 95-05 (1995).
- [5] B. E. Carlsten and T. O. Raubenheimer, *Phys. Rev. E* **51**, 1453 (1995).
- [6] E.D. Courant and H.S. Snyder, *Annals of Phys.* **3**, 1 (1958).
- [7] D. Douglas, JLAB-TN-98-012 (1998).
- [8] P. Emma and R. Brinkmann, SLAC-PUB-7554 (1997).
- [9] E.L. Saldin, E.A. Schneidmiller, and M.V. Yurkov, *Nucl. Instrum. Methods Phys. Res., Sect. A* **398**, 373 (1997).
- [10] E. Allaria et al., *Nat. Photon.* **6** (2012) 699–704.
- [11] E. Allaria et al., *Nat. Photon.* **7** (2013) 913–918.
- [12] S. Di Mitri, M. Cornacchia and S. Spampinati, *Phys. Rev. Letters* **110**, 014801 (2013).
- [13] S. Di Mitri, M. Cornacchia, *Europhys. Letters* **109**, 62002 (2015).
- [14] M. Borland, APS Tech Note LS-207 (2000).
- [15] Y. Jiao, X. Cui, X. Huang and G. Xu, *Phys. Rev. Special Topics – Accel. Beams* **17**, 060701 (2014).
- [16] S.V. Benson et al., *Journal of Modern Optics*, **58**:16, 1438-1451 (2011).
- [17] P. Piot, D. R. Douglas, and G. A. Krafft, *Phys. Rev. Special Topics – Accel. Beams*, **6**, 030702 (2003).
- [18] G.H. Hoffstaetter and Y. H. Lau, *Phys. Rev. Special Topics – Accel. Beams*, **11**, 070701 (2008).
- [19] D.R. Douglas et al., Thomas Jefferson National Accelerator Facility Report No. JLAB-ACP-14-1751 (2014), arXiv:1403.2318.
- [20] Y. Jing, Y. Hao and V. N. Litvinenko, *Phys. Rev. Special Topics – Accel. Beams*, **16**, 060704 (2013).
- [21] J.H. Wu, J.B. Murphy, V. Yakimenko, I. Ben-Zvi, W. Graves, E. Johnson, S. Krinsky and T. Shaftan, in *Proc. of the 2001 Part. Accel. Conf.*, RPAH012, edited by P.W. Lucas and S. Webber, Chicago, IL, U.S.A. (2001).
- [22] R. Hajima, *Nucl. Instrum. Meth. Phys. Research, Sect. A* **528**, 335 (2004).
- [23] M. Shimada, K. Yokoya, T. Suwada and A. Enomoto, *Nucl. Instrum. Meth. Phys. Research, Sect. A* **575**, 315 (2007).
- [24] M. Borland and V. Sajaev, in *Proc. of the 24th Linear Accel. Conf.*, TUP023, edited by B. Laxdal and P.W. Schmor, Victoria, BC, Canada (2008).
- [25] S. Di Mitri and M. Cornacchia, *Nucl. Instrum. Meth. Phys. Research, Sect. A* **735**, 60 (2014).
- [26] R.C. York, *Phys. Rev. Special Topics – Accel. Beams* **17**, 010705 (2014).
- [27] R. Bonifacio, C. Pellegrini and L. Narducci, *Opt. Commun.* **50**, 373-378 (1984).
- [28] M. Xie, in *Proc. of 1995 Part. Accel. Conf.*, Dallas, TX, USA, IEEE, 183–185 (1995).